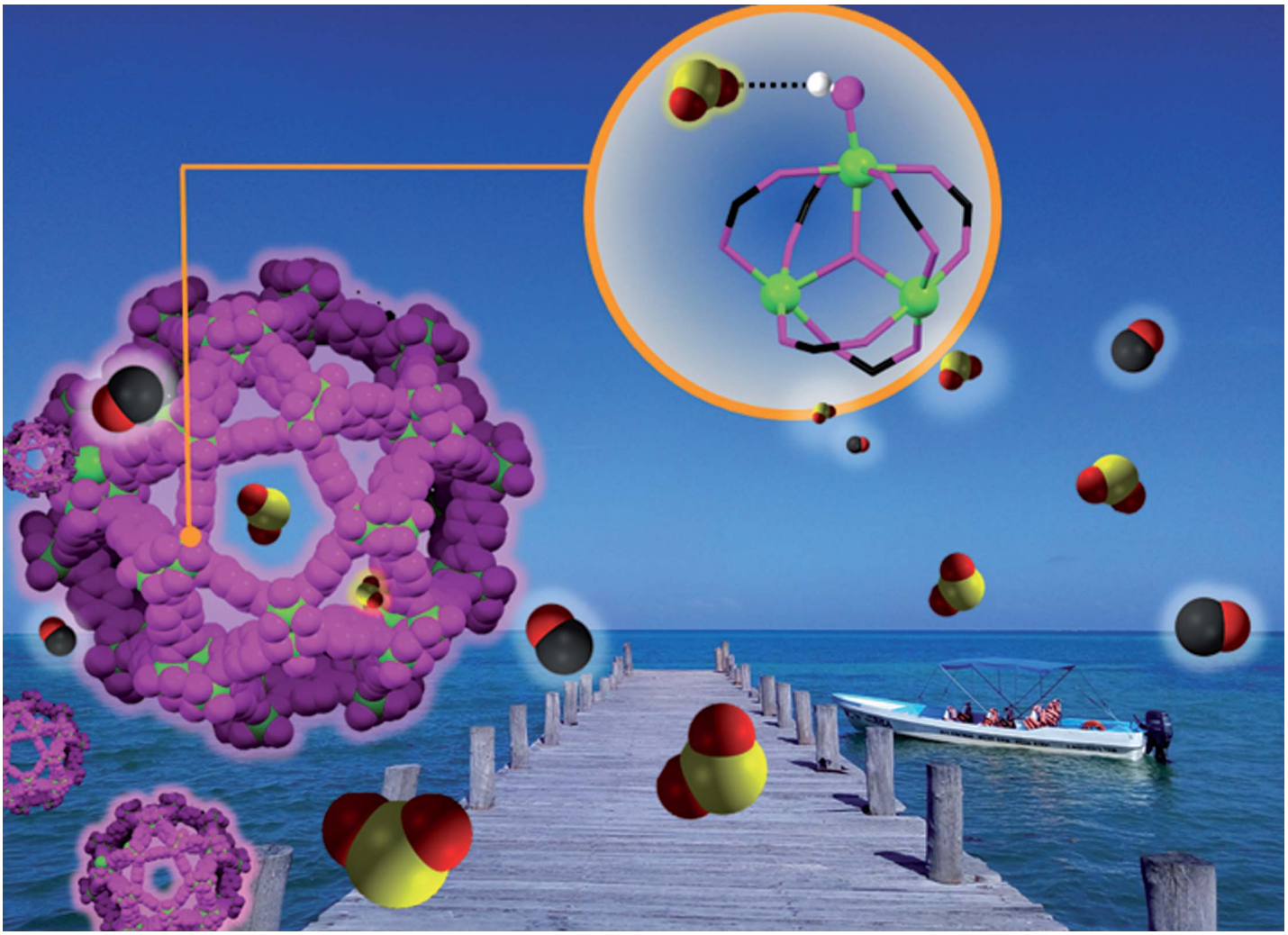

**Showcasing research from Prof. Enrique Lima and Prof. Ilich A. Ibarra, Instituto de Investigaciones en Materiales (IIM), from The National Autonomous University of Mexico (UNAM), Ciudad de México, Mexico.**

High and reversible $SO_2$ capture by a chemically stable Cr(III)-based MOF

A partially fluorinated MOF material named MIL-101(Cr)-4f(1%) exhibits high $SO_2$ capture, high chemical stability towards dry and humid $SO_2$ and outstanding cycling performance with facile regeneration.

## As featured in:


See Enrique Lima, Ilich A. Ibarra *et al.*, *J. Mater. Chem. A*, 2020, **8**, 11515.

ROYAL SOCIETY OF CHEMISTRY

rsc.li/materials-a

Registered charity number: 207890

Journal of Materials Chemistry A

ROYAL SOCIETY OF CHEMISTRY

COMMUNICATION

View Article Online
View Journal | View Issue



Cite this: J. Mater. Chem. A, 2020, 8, 11515

Received 10th December 2019
Accepted 9th April 2020

DOI: 10.1039/c9ta13524c

rsc.li/materials-a



# High and reversible $SO_2$ capture by a chemically stable Cr(III)-based MOF†

Eva Martínez-Ahumada,‡[a] Mariana L. Díaz-Ramírez,‡[a] Hugo A. Lara-García,[b] Daryl R. Williams,[c] Vladimir Martis,[d] Vojtech Jancik,[ef] Enrique Lima*[a] and Ilich A. Ibarra*[a]

Partially fluorinated MIL-101(Cr) shows high $SO_2$ capture (up to 18.4 mmol $g^{-1}$ at 298 K and up to 1 bar), chemical stability towards dry and humid $SO_2$ and an outstanding cycling performance with facile regeneration. *In situ* DRIFT spectroscopy demonstrated the preferential adsorption sites within MIL-101(Cr)-4F(1%).

## Introduction

Sulphur dioxide ($SO_2$) is a toxic gas with a pungent odour. Although it is naturally produced by volcanic activity, its main source is the burning of fossil fuels containing sulphur and metal extraction from ores.[1] This gas has been labelled by the World Health Organization (WHO) as one of the most hazardous air pollutants as its presence has been correlated with a rise in respiratory problems[2,3] and mortality.[4] It is also a precursor of particulate matter (PM), which also poses a threat to human health.[5] Furthermore, $SO_2$ is one of the main components of acid deposition which affects aquatic environments and causes loss of minerals and nutrients from the soil, hindering the growth of forests and crop plants.[6] Therefore, in order to improve the quality of air, especially in urban areas, emissions of $SO_2$ should be reduced.

The most used devices for $SO_2$ removal from industrial combustion units are scrubbers,[7] where an alkaline reagent (typically lime or limestone) is used to produce a solid compound (calcium sulphite). Nevertheless, this technology has some drawbacks such as low capture of $SO_2$, corrosion of pipelines and substantial cost of use and recovery.

The removal of this gas has also been explored in porous materials such as zeolites,[8,9] which have basic oxygen atoms on the surface that make them good candidates for $SO_2$ capture. However, the regeneration process requires heating above 450 °C (ref. 10) or a chemical treatment with hydrogen peroxide,[11] which may lead to a modification of the structure and a loss of porosity of the zeolites, rendering them non-reusable.

The capture of an acidic gas such as $SO_2$ has proved to be a difficult task because of the formation of strong irreversible interactions (chemisorption) or a highly expensive regeneration process of the material used. Therefore, it is fundamental to find more efficient and effective $SO_2$ removal technologies. As an alternative, a new class of crystalline and porous materials known as porous coordination polymers (PCPs) or metal–organic frameworks (MOFs) has been explored. MOFs are formed by organic linkers (typically carboxylic acids or azo-ligands)[12] and metal ions or metal-oxide clusters,[13] giving rise to one-, two- or three-dimensional arrays, depending on the type of the linker and the metal centre used. The properties of these materials, such as adsorption capacity or selectivity towards specific molecules, can be finely customised by changing the metal centre or by adding a chemical functionality to the linker.

Some studies have demonstrated the capture of sulphur-oxide gases by different MOFs; however, only a few of them have shown to be stable upon $SO_2$ exposure. This is because of the strong interaction between the metal centre and $SO_2$, which can break metal–ligand bonds causing structural degradation or collapse, as shown for MOF-177,[14] which, although holding the record for $SO_2$ capture (25.7 mmol $g^{-1}$ at 298 K and 1 bar),

[a]Laboratorio de Fisicoquímica y Reactividad de Superficies (LaFReS), Instituto de Investigaciones en Materiales, Universidad Nacional Autónoma de México, Circuito Exterior s/n, CU, Coyoacán, 04510, Ciudad de México, Mexico. E-mail: lima@iim.unam.mx; argel@unam.mx; Fax: +52(55) 5622-4595

[b]Instituto de Física, Universidad Nacional Autónoma de México, Circuito de la Investigación Científica s/n, CU, Coyoacán, Ciudad de México, Mexico

[c]Surfaces and Particle Engineering Laboratory (SPEL), Department of Chemical Engineering, Imperial College London, South Kensington Campus, London SW7 2AZ, UK

[d]Surface Measurement Systems, Unit 5, Wharfside, Rosemont Road, London HA0 4PE, UK

[e]Universidad Nacional Autónoma de México, Instituto de Química, Ciudad Universitaria, Ciudad de México, 04510, Mexico

[f]Centro Conjunto de Investigación en Química Sustentable UAEM-UNAM, Carr. Toluca-Atlacomulco Km 14.5, Toluca, Estado de México 50200, Mexico

† Electronic supplementary information (ESI) available. See DOI: 10.1039/c9ta13524c

‡ These authors contributed equally to this work.

showed changes in crystallinity and loss of BET surface area after $SO_2$ adsorption. To avoid this, the interactions between $SO_2$ and the MOF material should be through a donor–acceptor bond with open metal sites or *via* non-covalent bonding between $SO_2$ and ligands. For instance, several studies have been performed exploring the hydrogen bond formation as the main interaction between $SO_2$ and MOFs, using, for example, linkers with urea groups[15] or through μ-OH groups.[14,16–19]

There are remarkable examples showing that the existence of open metal sites favours the affinity towards polar molecules such as $SO_2$.[20] Nonetheless, humid conditions have exhibited an unfavourable impact on the capture of $SO_2$, due to (i) the competition of $H_2O$ and $SO_2$ molecules for the preferential adsorption sites (*i.e.*, open metal sites)[21] and (ii) the chemical reaction of $H_2O$ and $SO_2$ to form highly reactive sulphurous acid ($H_2SO_3$), capable of degrading MOF materials.[14] DFT calculations have provided valuable information to understand how open metal sites interact with guest molecules, finding that the primary interaction is between one oxygen atom from the $SO_2$ molecule and the metal centre; for example, Mg- and Zn-MOF-74.[22]

The introduction of highly electronegative atoms such as fluorine in the structure of MOFs has also shown interesting results for the capture of $SO_2$. For example, using an inorganic anion ($SIF_6^{2-}$, SIFSIX) pillared metal–organic framework, Xing and co-workers[23] identified that the main interactions of $SO_2$ with the framework is through guest–host electrostatic interactions such as $S^{\delta+}\cdots F^{\delta-}$ and OS–O$\cdots$H–C (ligand). These interactions firmly bind $SO_2$ in the pores of the materials. Moreover, guest–guest interactions ($OS_1$–O$\cdots S_2$–O) allowed a more ordered packing of $SO_2$ within the pore, forming a $SO_2$ cluster. Also, considering the interaction $S^{\delta+}\cdots F^{\delta-}$ – as a good site for $SO_2$ adsorption, Eddaoudi *et al.*[24] studied the $SO_2$ capture in two isostructural fluorinated MOFs, namely, KAUST-7 and KAUST-8. Interestingly, both materials have excellent stability towards moisture and can be easily regenerated.

Recently, we have reported a partially fluorinated version of MIL-101(Cr) entitled MIL-101(Cr)-4F(1%)[25] that showed interesting adsorption properties for different analytes ($H_2O$, $CO_2$, $O_2$, $H_2$ and $H_2S$). Particularly, we demonstrated that fluorine incorporation promoted a higher acidity of some of the Cr(III) metal centres (open metal sites), due to the capability of fluorine to attract electrons.[25] Thus, in this contribution we present the remarkable capture of $SO_2$ on this partially fluorinated material, the chemical stability of MIL-101(Cr)-4F(1%) towards $SO_2$ (under both dry and humid conditions), and the relevance of the open metal sites of MIL-101(Cr)-4F(1%) for high $SO_2$ capture demonstrated by *in situ* DRIFTS CO adsorption experiments. Remarkable MOF examples capable of adsorbing $SO_2$ at very low pressures (since the concentration of atmospheric $SO_2$ is very low) have been reported.[17,23] Although, $SO_2$ capture in these conditions for MIL-101(Cr)-4F(1%) is not outstanding, our material could be an exceptional alternative for $SO_2$ long-term storage.

Powder X-ray diffraction (PXRD) confirmed the phase purity of MIL-101(Cr)-4F(1%) and thermogravimetric analysis (TGA) confirmed the previously reported decomposition temperature[25] (see Experimental details, Fig. S1 and S5, ESI†). Acetone-exchanged samples of MIL-101(Cr)-4F(1%) were fully activated (see the Experimental section, ESI†) and an $N_2$ isotherm at 77 K demonstrated a BET surface area of 2176 $m^2$ $g^{-1}$ with a pore volume of 1.19 $cm^3$ $g^{-1}$ (see Fig. S6, ESI†).

Then, $SO_2$ adsorption–desorption isotherms using a Dynamic Gravimetric Gas/Vapour Sorption Analyser, DVS vacuum (Surface Measurement Systems Ltd), were carried out from 0 to 1 bar at 298 K on an activated sample (see the ESI†) of MIL-101(Cr)-4F(1%). Fig. 1 shows the resulting isotherm that was observed, which shows a rapid $SO_2$ uptake from 0.0 to 0.1 bar with a total uptake of approximately 4.6 mmol $g^{-1}$ (see the inset of Fig. 1). From 0.1 to 0.2 bar the $SO_2$ adsorption isotherm demonstrated an almost linear uptake with a total amount of $\approx$7.5 mmol $g^{-1}$. Finally, from 0.2 to 1.0 bar (end of the experiment) an exceptional $SO_2$ total uptake of 18.4 mmol $g^{-1}$ was achieved. This value is higher than the $SO_2$ capture for representative MOFs (*e.g.*, SIFSIX-1-Cu[23] = 11.0 mmol $SO_2$ $g^{-1}$, and, very recently, MFM-170 (ref. 26) = 17.5 mmol $g^{-1}$, at 298 K and up to 1 bar). It also signifies the second highest $SO_2$ uptake for a MOF material. Interestingly, MOF-177 (ref. 14) demonstrated the highest $SO_2$ uptake for a MOF, reported to date, with a total capture of 25.7 mmol $g^{-1}$ with an estimated BET surface area of 4100 $m^2$ $g^{-1}$, whereas the BET surface area for MIL-101(Cr)-4F(1%) (2176 $m^2$ $g^{-1}$) is approximately 47% lower than MOF-177. However, when MOF-177 was tested for a second $SO_2$ re-adsorption experiment (first cycle), this material showed partial degradation of the framework structure (corroborated by PXRD) and reduction of the BET surface area (2270 $m^2$ $g^{-1}$). Therefore, because of the low chemical stability of MOF-177, no further $SO_2$ sorption investigations for MOF-177 were considered by the authors.[14]

Thus, we decided to investigate the structural stability of MIL-101(Cr)-4F(1%) after the $SO_2$ adsorption–desorption experiment. PXRD analysis confirmed the retention of its crystallinity (see Fig. S2, ESI†), after the first $SO_2$ sorption experiment. In addition, a $N_2$ adsorption at 77 K evidenced that the

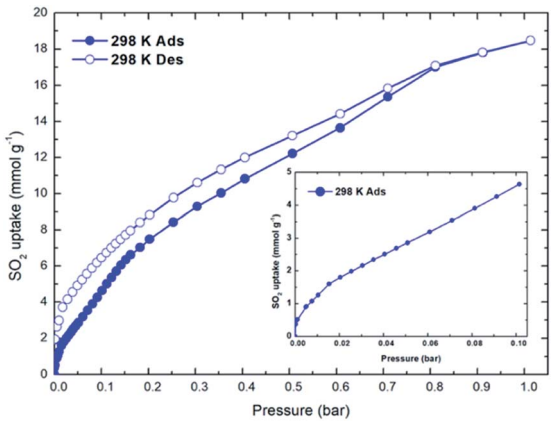


Fig. 1 Experimental $SO_2$ adsorption–desorption isotherm collected for a fully activated MIL-101(Cr)-4F(1%) sample (filled blue circles = adsorption; open blue circles = desorption) at 298 K and up to 1 bar. Inset: $SO_2$ adsorption from 0.0 to 0.1 bar.

 

porosity was not altered (BET area ≈ 2168 $m^2$ $g^{-1}$, see Fig. S7, ESI†). Continuing with the analysis of the $SO_2$ sorption isotherm, the desorption branch showed a hysteresis from 0.8 bar to 0.0 bar which indicates a relatively strong $SO_2$ interaction with the MOF material.

In order to quantify such a host–guest interaction, the isosteric heat of adsorption ($\Delta H$) was evaluated for $SO_2$ at low coverage for fully activated MIL-101(Cr)-4F(1%) (estimated by fitting three adsorption isotherms at 298, 303 and 308 K to a Clausius–Clapeyron equation, see Fig. S11, ESI†). Thus, the resultant $\Delta H = -54.3$ kJ $mol^{-1}$ was demonstrated to be relatively high which is consistent with the hysteresis shown in Fig. 1 (suggesting a relatively strong interaction between $SO_2$ and the MOF material). This $\Delta H$ value is characteristic for $SO_2$ and open metal sites systems (*e.g.*, KAUST-8,[24] $\Delta H = -73.9$ kJ $mol^{-1}$).

Cycling $SO_2$ experiments at 298 K and 1 bar were further carried out in order to assess the stability of the $SO_2$ adsorption performances and the regeneration capacity of MIL-101(Cr)-4F(1%). We recently reported the $SO_2$ cyclability of MFM-300(Sc),[27] where only vacuum ($1.7 \times 10^{-6}$ Torr) was applied for 30 minutes at 298 K. Since the $\Delta H$ for $SO_2$ in MFM-300(Sc) ($-36.2$ kJ $mol^{-1}$) resulted in a lower value than that for MIL-101(Cr)-4F(1%) ($-54.3$ kJ $mol^{-1}$), we decided to carry out cycling $SO_2$ experiments on MIL-101(Cr)-4F(1%) by applying vacuum ($1.7 \times 10^{-6}$ Torr) for 45 minutes and 298 K. Thus, we demonstrated that the $SO_2$ capture capacity remains constant during 50 adsorption–desorption cycles (18.44 ± 0.12 mmol $g^{-1}$, see Fig. 2). This shows that $SO_2$ is fully released during the subsequent desorption cycles. PXRD analyses of the material after 50 adsorption/desorption cycles confirmed the retention of the crystal structure (see Fig. S3, ESI†), while a $N_2$ adsorption at 77 K evidenced that the porosity is not altered (BET area ≈ 2174 $m^2$ $g^{-1}$) (see Fig. S8, ESI†). Additionally, *in situ* PXRD (under a $N_2$ atmosphere) demonstrated that this $SO_2$ re-cycled material retained its crystallinity up to 250 °C (see Fig. S4, ESI†). MIL-101(Cr)-4F(1%) shows a fast reactivation process (treatment for 45 min under vacuum) at room temperature (298 K) which contrasts with the harsh conditions currently considered for most of the current MOFs envisaged for $SO_2$ capture.[28]

MFM-170, with a BET surface area of 2408 $m^2$ $g^{-1}$, exhibited the highest $SO_2$ uptake (17.5 mmol $g^{-1}$, at 1 bar and 298 K), reported in the literature, for a chemically stable MOF material (50 adsorption–desorption cycles for $SO_2$ at 298 K under dynamic vacuum).[26] Therefore, MIL-101(Cr)-4F(1%) represents the highest $SO_2$ capture (18.4 mmol $g^{-1}$) in a chemically stable MOF material with an extraordinary energy-efficient cyclability.

Taking into account the excellent water stability of MIL-101(Cr)-4F(1%)[25] and the chemical stability towards $SO_2$, no loss of the adsorption capacity of $SO_2$ after 50 adsorption–desorption cycles and PXRD confirmation of the crystalline structure, the structure stability of MIL-101(Cr)-4F(1%) towards humid $SO_2$ was investigated. Then, an activated sample (see the ESI†) of MIL-101(Cr)-4F(1%) was exposed during 24 h to humid $SO_2$ (60% relative humidity, RH), generated in a home-designed set-up (see Fig. S13, ESI†). Later, this sample was re-activated (as previously described in the ESI†) and it was re-exposed to humid $SO_2$ for another 24 h (second exposure to humid $SO_2$). After completing a third exposure to humid $SO_2$ (60% RH), PXRD experiments demonstrated the retention of the crystallinity of the sample (see Fig. 3) and a $N_2$ adsorption at 77 K showed that the porosity was not altered (BET area ≈ 2172 $m^2$ $g^{-1}$, see Fig. S9, ESI†). These cycling experiments with humid $SO_2$ demonstrated the high chemical stability of MIL-101(Cr)-4F(1%).

Up to this point we have demonstrated that the $SO_2$ capture by MIL-101(Cr)-4F(1%) is the highest, to the best of our knowledge, for a structurally stable MOF material, with high $SO_2$ cyclability and extraordinary chemical stability towards humid $SO_2$. When comparing MIL-101(Cr)-4F(1%) to MFM-170,[26] the latter shows higher BET surface area (2176 *vs.* 2408 $m^2$ $g^{-1}$) and pore volume (0.88 *vs.* 1.19 $cm^3$ $g^{-1}$). Although, the pore dimensions of MFM-170 belong to the mesoporous regime (three different cavities: A (15.9 Å), B (16.3 × 22.2 Å) and C (12.8 × 14.2 Å)), similar to those of MIL-101(Cr)-4F(1%) with two different pore openings (29 Å and 34 Å), the total uptake is higher for MIL-101(Cr)-4F(1%). Thus, the difference in the $SO_2$ capture for these two materials cannot be simply explained by

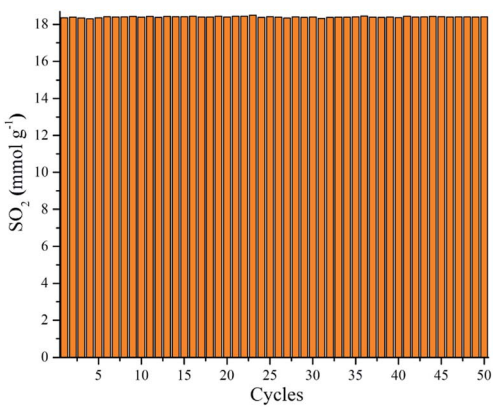


Fig. 2 Adsorption–desorption cycles for $SO_2$ in MIL-101(Cr)-4F(1%) at 1 bar and 298 K. The re-activation of this sample was conducted by only applying vacuum ($1.7 \times 10^{-6}$ Torr) for 45 minutes at 298 K.

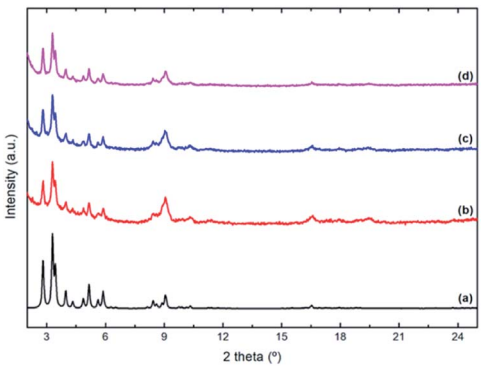


Fig. 3 PXRD of (a) simulated MIL-101(Cr)-4F(1%), (b) first, (c) second, and (d) third exposure to humid $SO_2$.

their porosity differences. In addition, both mesoporous MOF materials show access to open metal sites.

However, the $\Delta H$ for $SO_2$ (at low $SO_2$ loadings) was demonstrated to be considerably different for MIL-101(Cr)-4F(1%) ($-54.3$ kJ mol$^{-1}$) and MFM-170 ($-35.4$ kJ mol$^{-1}$).[26] Since this parameter is calculated at low $SO_2$ loadings, it indicates the interaction of the $SO_2$ molecules with the preferential functional groups within a MOF material, which are in the case of MIL-101(Cr)-4F(1%) and MFM-170 the open metal sites (Cr(III) and Cu(II), respectively). Thus, we hypothesise that due to a higher $\Delta H$ for $SO_2$ for MIL-101(Cr)-4F(1%), the $SO_2$ uptake is accordingly higher, presumably due to a more efficient packing of the $SO_2$ molecules. In order to corroborate our hypothesis, Diffuse Reflectance Infrared Fourier Transform (DRIFT) spectroscopy experiments were performed. Indeed, Yang and Schröder elegantly demonstrated (by *in situ* synchrotron single-crystal X-ray diffraction) the binding domains for adsorbed $SO_2$ within MFM-170 (open metal sites).[26] In our hands, we investigated such binding domains by *in situ* DRIFT spectroscopy upon the adsorption of CO. Although CO is chemically different from $SO_2$, both molecules exhibit a dipole moment (D, 0.12 for CO and 1.62 for $SO_2$) and we decided to use this molecule as a probe, affording an extraordinary alternative to investigate the preferential adsorption sites within MIL-101(Cr)-4F(1%). CO is indeed an IR probe that can be used to characterise the acidity of surfaces. Therefore, CO was selected as a good candidate since $SO_2$, also a dipolar molecule, is anticipated to be adsorbed at acid sites similar to CO.

Fig. 4 shows the spectra of CO adsorption (298 K) at different times (min) on an activated sample (see the ESI†) of MIL-101(Cr)-4F(1%). After only 1 min, the CO adsorption showed two bands centred at $\tilde{\nu}$ 2191 and 2161 cm$^{-1}$. In line with the earlier-observed cation-dependent vibrational band,[29] the main band at $\tilde{\nu}$ 2191 cm$^{-1}$ is attributed to CO interacting with the Lewis $Cr^{3+}$ sites, confirming that the $Cr^{3+}$ are indeed open metal sites

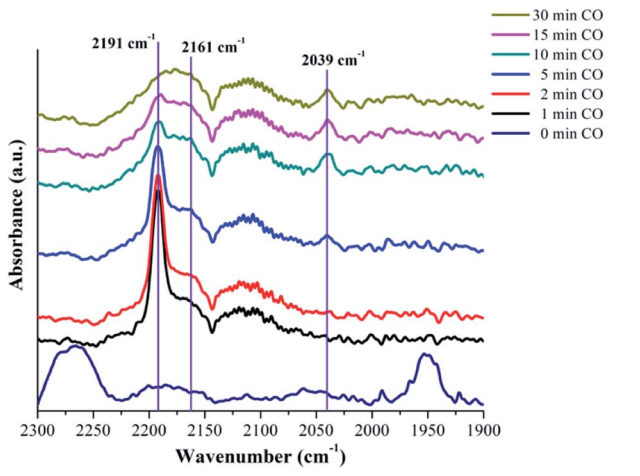


Fig. 4 DRIFT spectroscopy spectra of CO adsorbed at different times over activated MIL-101(Cr)-4F(1%) at 298 K, in the region between $\tilde{\nu}$ 2300 and 1900 cm$^{-1}$. At 0 min, the DRIFT spectroscopy spectrum of MIL-101(Cr)-4F(1%) is shown; from 1 min to 30 min the DRIFT spectroscopy difference spectra are shown.

as previously demonstrated by $^{129}$Xe NMR.[25] Interestingly, the band at 2161 cm$^{-1}$ is assigned to CO interacting with Brönsted acid sites (hydrogen atom from the HO group) (see Fig. S14, ESI†). In both cases the positions shift (approximately 6 cm$^{-1}$ for $\tilde{\nu}$ 2191 cm$^{-1}$ and 4 cm$^{-1}$ for $\tilde{\nu}$ 2161 cm$^{-1}$) as time increases (coverage-dependent) and undoubtedly, these are distinct from the previously reported gas-phase band observed at $\tilde{\nu}$ 2143 cm$^{-1}$.[29] In fact, the coverage-dependent shift ($\sim$6 cm$^{-1}$) for the main band (2191 cm$^{-1}$) is attributed to additional CO–CO lateral interactions since CO is a small polarisable molecule (*i.e.*, exhibits a dipole moment). This high value (main band at $\tilde{\nu}$ 2191 cm$^{-1}$) of the CO stretching frequency and the very small shift (6 cm$^{-1}$) of this band as CO coverage evolves suggests a poor or negligible participation of the d-$\pi$* orbital in the interaction between $Cr^{3+}$ and CO.[30] Consequently, the adsorption of CO on these sites ($Cr^{3+}$) of the material can be considered as relatively weak.

Additionally, after 5 min a band is observed at 2039 cm$^{-1}$, which is a significantly lower wave number than the one observed for CO adsorbed within other MOF materials.[31] In fact, this band is also at a lower wave number than that expected for CO interacting with $Cr^{3+}$ or Brönsted acid sites as previously identified.[30] This band is indeed close to the one previously observed for CO bonded to metal chromium ($Cr^0$) in carbonyl complexes.[32] However, this can be discarded as the reduction from $Cr^{3+}$ to $Cr^0$ did not take place in MIL-101(Cr)-4F(1%). Interestingly, it is possible to decrease the strength of the triple polar-covalent bond between C and O atoms of the CO molecule (C$\equiv$O), if it is exposed to two different interactions.[33]

Thus, we hypothesise that when the CO molecule is adsorbed within MIL-101(Cr)-4F(1%), after a particular CO concentration is reached (*i.e.*, after 5 min, see Fig. 4 band at $\tilde{\nu}$ 2039 cm$^{-1}$), a specific adsorbed geometry is afforded which allows the CO molecule to simultaneously interact with coordinative unsaturated $Cr^{3+}$ metal centres (Lewis acid sites) and OH functional groups (Brönsted acid sites) (see Fig. S15, ESI†). Both interactions (depicted as: O–H$\cdots$O$\equiv$C–Cr) can generate a weakening of the triple bond of the CO molecule and therefore, a higher stabilisation of this molecule within the MOF material. This experimental evidence can be observed in Fig. 4 where from 5 min to 30 min (end of the experiment), the intensity of the main band at $\tilde{\nu}$ 2191 cm$^{-1}$ is considerably broadened and shifted ($\sim$6 cm$^{-1}$) while the intensity of the dually interacting band (O–H$\cdots$O$\equiv$C–Cr) at $\tilde{\nu}$ 2039 cm$^{-1}$, is increased. Furthermore, changes observed in the $\nu_{OH}$ region (see Fig. S12, ESI†) provided a clear evidence of hydrogen bond formation (O–H$\cdots$O$\equiv$C). After only 2 min of CO adsorption, the main bands at $\tilde{\nu}$ 3665 and 3585 cm$^{-1}$ were considerably broadened and shifted slightly to lower wavenumbers and a new band at $\tilde{\nu}$ 3612 cm$^{-1}$ was observed (see Fig. S12, ESI†). These adsorption sites in which CO is simultaneously bounded to OH and $Cr^{3+}$, significantly decrease the strength of the triple polar-covalent bond of CO, and therefore, these can be considered as strong adsorption sites for CO.

All the previously analysed vibrational bands (DRIFT spectroscopy spectra) correspond to the chemical composition of activated MIL-101(Cr)-4F(1%): $[Cr_3O(BDC)_{2.91}(BDC\text{-}4)_{0.09}(H_2O)\cdot$

 

OH]; BDC = 1,4-benzenedicarboxylate; BDC-4F = 2,3,5,6-tetrafluoro-1,4-benzenedicarboxylate (see ESI,† material synthesis). In detail, the trinuclear cluster $Cr_3O$ of Cr(III) is coordinated to two $H_2O$ molecules and one hydroxy group (HO) (this anion compensates the charge of the framework structure). Upon activation, these water molecules are displaced generating open metal sites and the HO remains coordinated to one metal centre (see Fig. S14, ESI†).[34] Thus, as previously described (*vide supra*), this HO functional group (Brönsted acid site) is the one responsible (in combination with unsaturated $Cr^{3+}$, a Lewis acid site) for the simultaneous CO interaction with both adsorption sites as evidenced by the band at $\tilde{\nu}$ 2039 $cm^{-1}$ and the changes observed in the $\nu_{OH}$ region. Thus, with this experimental evidence, we corroborated our efficiently packing $SO_2$ hypothesis: the $SO_2$ adsorption process takes place in three stages: (i) adsorption at acid sites (Lewis) with a relatively high $\Delta H$ for $SO_2$; (ii) adsorption at both acid (Lewis and Brönsted) sites, since the $SO_2$ molecule also exhibits a dipole moment (resembling the CO molecule) and (iii) adsorption within the cavities of the MOF material.

To summarise, MIL-101(Cr)-4F(1%) exhibits the highest $SO_2$ uptake for a structurally stable MOF material, extraordinary chemical stability towards dry and humid $SO_2$ and an excellent cycling performance with facile regeneration at room temperature. Furthermore, *in situ* DRIFT spectroscopy upon the adsorption of CO identified the preferential adsorption sites of MIL-101(Cr)-4F(1%).

## Conflicts of interest

There are no conflicts to declare.

## Acknowledgements

The authors thank Dr A. Tejeda-Cruz (powder X-ray; IIM-UNAM), CONACyT (1789), and the PAPIIT UNAM (IN101517, IN202820), México for financial support. E. M.-A. acknowledges a Ph.D. CONACyT grant (770954). The authors thank U. Winnberg (ITAM) for scientific discussions and G. Ibarra-Winnberg for conceptualising the design of this contribution.

## Notes and references

1 Z. Klimont, S. J. Smith and J. Cofala, *Environ. Res. Lett.*, 2013, **8**, 014003.
2 M. Matooane and R. Diab, *Arch. Environ. Health*, 2003, **58**, 763–770.
3 P. Amoatey, H. Omidvarborna, M. S. Baawain and A. Al-Mamun, *Process Saf. Environ. Prot.*, 2019, 215–228.
4 J. Schwartz and D. W. Dockery, *Am. Rev. Respir. Dis.*, 1992, **145**, 600–604.
5 R. Reiss, E. L. Anderson, C. E. Cross, G. Hidy, D. Hoel, R. McClellan and S. Moolgavkar, *Inhalation Toxicol.*, 2007, **19**, 419–449.
6 F. C. Menz and H. M. Seip, *Environ. Sci. Policy*, 2004, **7**, 253–265.
7 R. K. Srivastava, W. Jozewicz and C. Singer, *Environ. Prog.*, 2001, **20**, 219–228.
8 B. E. Alver, M. Sakizci and E. Yörükoğullari, *Adsorpt. Sci. Technol.*, 2011, **29**, 413–422.
9 B. Erdoğan Alver, *J. Hazard. Mater.*, 2013, **262**, 627–633.
10 N. D. Hutson, B. A. Reisner, R. T. Yang and B. H. Toby, *Chem. Mater.*, 2000, **12**, 3020–3031.
11 A. J. Hernández-Maldonado, R. T. Yang, D. Chinn and C. L. Munson, *Langmuir*, 2003, **19**, 2193–2200.
12 W. Lu, Z. Wei, Z. Y. Gu, T. F. Liu, J. Park, J. Park, J. Tian, M. Zhang, Q. Zhang, T. Gentle, M. Bosch and H. C. Zhou, *Chem. Soc. Rev.*, 2014, **43**, 5561–5593.
13 R. F. Mendes and F. A. Almeida Paz, *Inorg. Chem. Front.*, 2015, **2**, 495–509.
14 P. Brandt, A. Nuhnen, M. Lange, J. Möllmer, O. Weingart and C. Janiak, *ACS Appl. Mater. Interfaces*, 2019, **11**(19), 17350–17358.
15 S. Glomb, D. Woschko, G. Makhloufi and C. Janiak, *ACS Appl. Mater. Interfaces*, 2017, **9**, 37419–37434.
16 S. Yang, J. Sun, A. J. Ramirez-Cuesta, S. K. Callear, W. I. F. David, D. P. Anderson, R. Newby, A. J. Blake, J. E. Parker, C. C. Tang and M. Schröder, *Nat. Chem.*, 2012, **4**, 887–894.
17 M. Savage, Y. Cheng, T. L. Easun, J. E. Eyley, S. P. Argent, M. R. Warren, W. Lewis, C. Murray, C. C. Tang, M. D. Frogley, G. Cinque, J. Sun, S. Rudić, R. T. Murden, M. J. Benham, A. N. Fitch, A. J. Blake, A. J. Ramirez-Cuesta, S. Yang and M. Schröder, *Adv. Mater.*, 2016, **28**, 8705–8711.
18 J. H. Carter, X. Han, F. Y. Moreau, I. Da Silva, A. Nevin, H. G. W. Godfrey, C. C. Tang, S. Yang and M. Schröder, *J. Am. Chem. Soc.*, 2018, **140**, 15564–15567.
19 L. Li, I. Da Silva, D. I. Kolokolov, X. Han, J. Li, G. Smith, Y. Cheng, L. L. Daemen, C. G. Morris, H. G. W. Godfrey, N. M. Jacques, X. Zhang, P. Manuel, M. D. Frogley, C. A. Murray, A. J. Ramirez-Cuesta, G. Cinque, C. C. Tang, A. G. Stepanov, S. Yang and M. Schröder, *Chem. Sci.*, 2019, **10**, 1472–1482.
20 D. Britt, D. Tranchemontagne and O. M. Yaghi, *Proc. Natl. Acad. Sci. U. S. A.*, 2008, **105**, 11623–11627.
21 T. Grant Glover, G. W. Peterson, B. J. Schindler, D. Britt and O. M. Yaghi, *Chem. Eng. Sci.*, 2011, **66**, 163–170.
22 K. Tan, S. Zuluaga, H. Wang, P. Canepa, K. Soliman, J. Cure, J. Li, T. Thonhauser and Y. J. Chabal, *Chem. Mater.*, 2017, **29**, 4227–4235.
23 X. Cui, Q. Yang, L. Yang, R. Krishna, Z. Zhang, Z. Bao, H. Wu, Q. Ren, W. Zhou, B. Chen and H. Xing, *Adv. Mater.*, 2017, **29**, 1606929.
24 M. R. Tchalala, P. M. Bhatt, K. N. Chappanda, S. R. Tavares, K. Adil, Y. Belmabkhout, A. Shkurenko, A. Cadiau, N. Heymans, G. De Weireld, G. Maurin, K. N. Salama and M. Eddaoudi, *Nat. Commun.*, 2019, **10**, 1328.
25 M. L. Díaz-Ramírez, E. Sánchez-González, J. R. Álvarez, G. A. González-Martínez, S. Horike, K. Kadota, K. Sumida, E. González-Zamora, M.-A. Springuel-Huet, A. Gutiérrez-Alejandre, V. Jancik, S. Furukawa, S. Kitagawa, I. A. Ibarra and E. Lima, *J. Mater. Chem. A*, 2019, **7**, 15101–15112.

26 G. L. Smith, J. E. Eyley, X. Han, X. Zhang, J. Li, N. M. Jacques, H. G. W. Godfrey, S. P. Argent, L. J. M. McPherson, S. J. Teat, Y. Cheng, M. D. Frogley, G. Cinque, S. J. Day, C. C. Tang, T. L. Easun, S. Rudić, A. J. Ramirez-Cuesta, S. Yang and M. Schröder, *Nat. Mater.*, 2019, **18**, 1358–1365.

27 J. A. Zárate, E. Sánchez-González, D. R. Williams, E. González-Zamora, V. Martis, A. Martínez, J. Balmaseda, G. Maurin and I. A. Ibarra, *J. Mater. Chem. A*, 2019, **7**, 15580–15584.

28 (*a*) L. M. Rodriguez-Albelo, E. Lopez-Maya, S. Hamad, A. R. Ruiz-Salvador, S. Calero and J. A. R. Navarro, *Nat. Commun.*, 2017, **8**, 1; (*b*) K. Tan, P. Canepa, Q. Gong, J. Liu, D. H. Johnson, A. Dyevoich, P. K. Thallapally, T. Thonhauser, J. Li and Y. J. Chabal, *Chem. Mater.*, 2013, **25**, 4653–4662; (*c*) X. Cui, Q. Yang, L. Yang, R. Krishna, Z. Zhang, Z. Bao, H. Wu, Q. Ren, W. Zhou, B. Chen and H. Xing, *Adv. Mater.*, 2017, **29**, 1606929.

29 K. Tan, S. Zuluaga, E. Fuentes, E. C. Mattson, J.-F. Veyan, H. Wang, J. Li, T. Thonhauser and Y. J. Chabal, *Nat. Commun.*, 2016, **7**, 13871.

30 (*a*) D. Scarano, A. Zecchina and A. Reller, *Surf. Sci.*, 1988, **198**, 11–25; (*b*) A. Vimont, H. Leclerc, F. Maugé, M. Daturi, J.-C. Lavalley, S. Surblé, C. Serre and G. Férey, *J. Phys. Chem. C*, 2007, **111**, 383–388.

31 (*a*) S. M. J. Rogge, A. Bavykina, J. Hajek, H. Garcia, A. I. Olivos-Suarez, A. Sepúlveda-Escribano, A. Vimont, G. Clet, P. Bazin, F. Kapteijn, M. Daturi, E. V. Ramos-Fernandez, F. X. L. i Xamena, V. Van Speybroeck and J. Gascon, *Chem. Soc. Rev.*, 2017, **46**, 3134–3184; (*b*) A. Vimont, J.-M. Goupil, J.-C. Lavalley, M. Daturi, S. Surblé, C. Serre, F. Millange, G. Férey and N. Audebrand, *J. Am. Chem. Soc.*, 2006, **128**(10), 3218–3227; (*c*) X. Li, T. W. Goh, L. Li, C. Xiao, Z. Guo, X. C. Zeng and W. Huang, *ACS Catal.*, 2016, **6**(6), 3461–3468.

32 Z. D. Reed and M. A. Duncan, *J. Am. Soc. Mass Spectrom.*, 2010, **21**, 739–749.

33 C. Otero Areán, G. Turnes Palomino, E. Escalona Platero and M. Peñarroya Mentruit, *J. Chem. Soc., Dalton Trans.*, 1997, 873–879.

34 G. Férey, C. Mellot-Draznieks, C. Serre, F. Millange, J. Dutour, S. Surblé and I. Margiolaki, *Science*, 2005, **309**, 2040.

 